Journal of Superconductivity and Novel Magnetism (2018) 31:2719–2732
https://doi.org/10.1007/s10948-017-4513-7

ORIGINAL PAPER

# Effects of Forming Pressure on Physicochemical Properties of YBCO Ceramics

**Pawel Peczkowski[1] · Piotr Szterner[1] · Zbigniew Jaegermann[1] · Marcin Kowalik[2] · Ryszard Zalecki[2] · Wieslaw Marek Woch[2]**

Received: 28 November 2017 / Accepted: 2 December 2017 / Published online: 13 January 2018


**Abstract**

This article details the solid-state synthesis of high-temperature superconducting $YBa_2Cu_3O_{7-x}$. Tests were carried out on samples formed at different pressures (200, 400, 600 and 800 MPa) before being annealed under pure oxygen. The X-ray diffraction method showed that, regardless of the forming pressure, the samples contain about 97 wt.% of Y-123 phase. SEM images showed a polycrystalline structure of samples of similar grain size and number of pores (intergranular spaces). The values of critical temperatures ($T_{c0}$), determined from magnetoresistance measurements, are about 91.5 K for all samples, and the $T_{c0}$ temperatures do not depend on sample-forming pressure. Magnetoresistance measurements have shown that samples formed with higher pressures exhibit smaller changes in $T_{c0}$ and superconducting transition width $\Delta T$ due to the influence of the $H_{DC}$ magnetic field, than the samples formed with lower pressures. Values of specific resistance determined by the use of van der Pauw method at 300 K is about 2 mΩcm for all samples. The critical temperatures ($T_c^{intra}$) of grains and critical current densities at 77 K were determined from AC magnetic susceptibility measurements, and they are about 91.6 K and 400 A $cm^{-2}$, respectively.

**Keywords** High-temperature superconductors (HTS) · YBCO · Forming pressure · Phase analysis

## 1 Introduction

Among superconductors, one can distinguish low-temperature superconductor (LTS), where superconductivity occurs at temperatures below 30 K, and high-temperature superconductors (HTS) having critical temperatures above 30 K. Over the last 30 years, many materials belonging to the high-temperature superconductor group have been discovered [1–7]. These superconductors, due to their electrical and magnetic properties, are a group of materials of great interest [8–11]. The interest was also due to the fact that the critical temperature was higher than the boiling point of liquid nitrogen. High-temperature superconductors are characterised by complex chemical composition. Their main ingredients are oxygen and copper; in smaller quantities, they contain bismuth, lead, thallium, mercury and lanthanides. In recent years, research has been focused on methods of obtaining and determining the physicochemical properties of $YBa_2Cu_3O_{7-x}$ (YBCO). The $YBa_2Cu_3O_{7-x}$ compound, also called Y-123 because of its stoichiometric composition, is one of the most important and most popular superconducting material [9].

Its advantage is a fairly high temperature of phase transition into superconducting state (about 93 K), which makes it possible to use it at liquid nitrogen temperatures [1]. The process of obtaining this superconductor is quite complex chemically [12].

It also requires maintaining a suitable temperature for a long time during the calcination processes in the air atmosphere and during annealing in pure oxygen atmosphere [12–16]. Currently, the work is focused on improving the efficiency of the process of obtaining this superconductor and reducing production costs. Many modifications of this process are also proposed, e.g., the

✉ Pawel Peczkowski
p.peczkowski@icimb.pl

[1] Department of Ceramic Technology, Institute of Ceramics and Building Materials, Postepu 9, 02-676 Warsaw, Poland

[2] Department of Solid State Physics, Faculty of Physics and Applied Computer Science, AGH University of Science and Technology, Adam Mickiewicz Avenue 30, 30-059 Cracow, Poland

use of weak microwaves during YBCO synthesis, the replacement of $BaCO_3$ with BaO [17].

In order to eliminate the formation of heterogeneous phase and loss of mass as a result of evaporation, several calcination methods are used: rapid [18], two-stage [19] and vacuum [20] calcinations. $YBa_2Cu_3O_{7-x}$ can be obtained at temperatures below 800 °C from oxides and carbonates by low-pressure oxygen calcination [21, 22]. In this way, it is possible to eliminate the non-superconductive phase that is formed at low temperatures. There has been virtually no works on the dependence of properties on the technological parameters of obtaining solid YBCO material. One of the few works is that of Ohmukai [17], which dealt with microwave annealing and studied the influence of pressure during YBCO molding in the range of 80–2000 kgf $cm^{-2}$ (about 7.8–196 MPa). He concluded that in order to minimise the undesirable phase of $BaCuO_2$ in YBCO, the pressure should be 700 kgf $cm^{-2}$ (about 68.6 MPa) [17].

Ohmukai [17] studied the effect of molding pressure on properties of the YBCO ceramics obtained during the use of the microwave method. Al-Shibani [23] studied the effect of molding pressure on the structural and physical properties of YBCO obtained by conventional calcination. Al-Shibani's paper [23] discussed the effect of forming pressure of samples on their critical temperature $T_c$ of their superconducting transition. Additionally, the author discussed the studies of resistance of the samples pressed under different pressures. The tests show the increase of the sample's resistance with increasing forming pressure.

Ohmukai's and Al-Shibani's researches have inspired the research team of the Institute of Ceramics and Building Materials in Warsaw trying to obtain a high-temperature ceramic superconductor $YBa_2Cu_3O_{7-x}$ and determine the dependence of its characteristics on the forming pressure of the material samples. To achieve this goal, a method of calcining a mixture of starting powders to obtain a superconducting material was used.

## 2 Materials Used

For high-temperature synthesis, the following starting powders (substrates) were used:

- Yttrium oxide(III)—$Y_2O_3$ from Alfa Aesar, purity 99.999%
- Barium carbonate—$BaCO_3$ from POCH, purity 99.6%,
- Copper(II) oxide—Alfa Aesar CuO, purity 99.999%.

The purity of the oxides used in this synthesis is very important. Trace amounts of other elements, especially ferromagnetic ones, can greatly reduce the critical temperature. The surface morphology of the substrates needed to make YBCO ceramics was evaluated using a scanning electron microscope. The microscope images shown in Fig. 1 indicate that the grains of yttrium oxide are non-homogeneous in shape and are cracked; the barium carbonate particles are longitudinal, while the copper oxide particles form very porous agglomerates.

The summary chemical equation (1) which describes the reaction of YBCO formation and which has been used to quantify the composition of raw materials is as follows:

$$Y_2O_3 + 4\,BaCO_3 + 6\,CuO \rightarrow 2\,YBa_2Cu_3O_{6.5} + 4\,CO_2\,(\uparrow)\,. \quad (1)$$

Table 1 gives an example of the composition of the set of substrates needed to obtain 50 g of $YBa_2Cu_3O_{6.5}$.

After weighing them with the accuracy of 0.0001 g, the $Y_2O_3$, $BaCO_3$ and CuO substrates were wet milled in the presence of isopropanol in a 1:1 powder/isopropanol ratio in a planetary mill for 75 min. The size of the grinders in 150 ml agate milling balls was between 15.0 and 19.7 mm, and the average size of the grinders was 17.24 ± 1.05 mm. Weights of single grinders in grinding balls ranged from 4.18 to 10.43 g, while the average weight was 7.25 ± 1.45 g. To analyse the dynamics of the milling process, slurry samples were taken for laser particle diffraction measurements every 15 min (Table 2). Based on own milling experience, it was found that the milling time of 75 min was sufficient both for the grinding of powders and their homogenisation.

## 3 Preparation of Test Samples

After milling and drying, the powder was placed in corundum crucibles and subjected to calcination processes for solid-phase reaction. Reactions in solid phase (first and second) were carried out in an electric muffle furnace (Fig. 2). Each of them consisted of the following stages:

1. Heating the powder to 950 °C for 5 h.
2. Annealing the powder to 950 °C for 24 h. During this annealing stage, an YBCO compound with perovskite structure is formed.
3. Cooling the powder to 400 °C for 3.5 h. This step prevents the rhombohedral phase from transforming into a tetragonal one.
4. Annealing at 400 °C for 24 h. During this stage, oxygen is drawn from the air.
5. Cooling the sample to room temperature.

After the first solid-phase reaction in air atmosphere, the mixture was comminuted in the presence of isopropanol in a proportion of 1:1 powder/isopropanol in a planetary mill for 210 min. After the first reaction in solid phase in the air atmosphere, the following granulations were obtained:

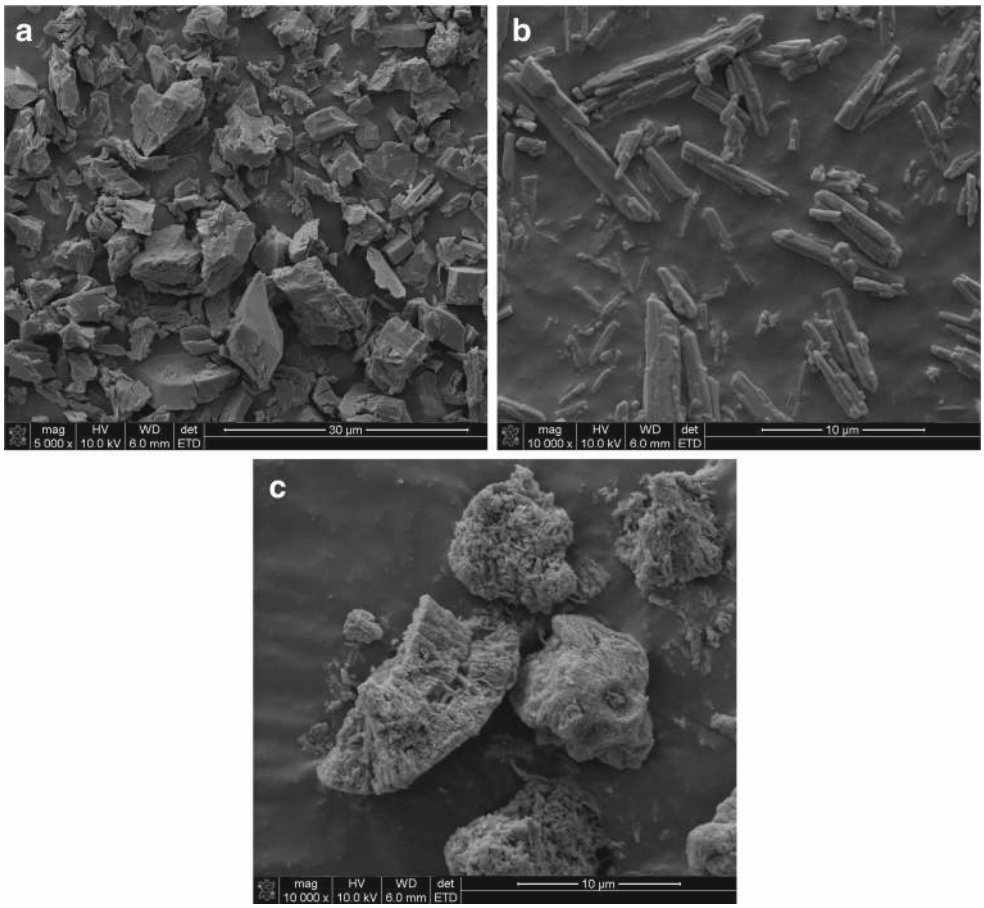


**Fig. 1** Images of substrate microstructure used for YBCO production (magnification, ×10,000): **a** $Y_2O_3$, **b** $BaCO_3$ and **c** CuO

$d$ (0.1) = 0.850, $d$ (0.5) = 3.519, and $d$ (0.9) = 12.658 µm. The mixture was also comminuted after the second reaction in solid phase, as before, in the presence of isopropanol in a ratio of 1:1 powder/isopropanol in a planetary mill for 210 min. After both first and second reaction processes in air atmosphere, we carried out a phase analysis of the powders obtained. Using the milled powders from first and second reactions in solid phase, we prepared two sets of test samples (A and B) obtained thanks to the axial pressing method with pressures of 200, 400, 600 and 800 MPa. The series A samples consisted of pellets with a diameter of about 12 mm, a weight of about 1 g and a height of about 2 mm, marked according to the pressures—200A, 400A, 600A and 800A. In contrast, the B series produced pellets with a diameter of about 12 mm, a weight of about 3 g and a height of about 6 mm, marked according to the pressures—200B, 400B, 600B and 800B. Each of the series was annealed in a separate process in an electric tube

**Table 1** Calculation of the composition of the set of substrates needed to obtain $YBa_2Cu_3O_{6.5}$

| Compound | $M$ (g mol$^{-1}$) | $M'$ (g mol$^{-1}$) | $K$ | $K/K_{YBCO}$ | Mass (g) |
|---|---|---|---|---|---|
| Substrates | | | | | |
| $Y_2O_3$ | 225.8100 | 225.8100 | 0.151304 | 0.171538 | 8.5769 |
| $BaCO_3$ | 197.3359 | 789.3436 | 0.528900 | 0.599628 | 29.9814 |
| CuO | 79.5454 | 477.2724 | 0.319796 | 0.362562 | 18.1281 |
| Products | | | | | |
| $YBa_2Cu_3O_{6.5}$ | 658.1940 | 1316.3880 | 0.882046 | 1 | 50.0000 |
| $CO_2$ | 44.0095 | 176.0380 | 0.117954 | – | 6.6864 |

$M$, molar mass; $M'$, molar mass multiplied by the stoichiometric coefficient; $K$, molar mass ratio (multiplied by the stoichiometric ratio) of a substrate or the total molar mass of the product; $K_{YBCO}$, molar mass ratio (multiplied by the stoichiometric ratio) of the substrate or product to the total YBCO molar mass

**Table 2** Results of grain size measurement of $Y_2O_3$, $BaCO_3$ and CuO

| Milling time (min) | Equivalent diameter of a grain $d$ (μm) | | |
|---|---|---|---|
| | $d$ (0.1) | $d$ (0.5) | $d$ (0.9) |
| 15 | 0.928 | 3.468 | 13.303 |
| 30 | 0.869 | 3.254 | 11.853 |
| 45 | 0.837 | 3.063 | 11.026 |
| 60 | 0.792 | 2.883 | 10.430 |
| 75 | 0.786 | 2.829 | 9.996 |

furnace. Series A pellets were stacked on three 10 × 10 cm alumina slabs, while batch B samples were stacked on one such plate. The plates were placed in the central part of the electric tube furnace (Fig. 3).

The annealing process was carried out in an atmosphere of flowing oxygen, which provided adequate doping of the samples with $O^{2-}$ ions. Oxygen was supplied to the furnace from the cylinder through a reducer and flowmeter (oxygen flow during the whole process was 20 l $h^{-1}$). The annealing process followed the curve shown in Fig. 4.

After the annealing process, the samples were placed in a desiccator to prevent them from aging due to air humidity.

## 4 Applied Testing Methods

The analysis of the grain size of the used raw materials was carried out using the low-angle laser light scattering (LALLS) method (also known as the laser diffraction method), with the use of a laser particle analyser with an attachment for preparation of samples in the form of dispersion in aqueous solutions or organic solvents.


**Fig. 2** Muffle furnace used for reaction in solid phase

**Fig. 3** Tube furnace for YBCO annealing in an oxygen atmosphere

Open porosity $P_o$, apparent density $dp$ and water absorption $N_w$ samples of YBCO material were determined by hydrostatic weighing in water using an analytical balance with an attachment for determining the density of solids. The calculations were made according to the following formulas:

$$P_o = \left( \frac{m_{ms} - m_{ds}}{m_{ms} - m_{inH_2O}} \right) \cdot 100\% \tag{2}$$

$$dp = \frac{m_{ds}}{m_{ms} - m_{inH_2O}} \tag{3}$$

$$N_w = \frac{m_{ds} - m_{ms}}{m_{ds}} \cdot 100\% \tag{4}$$

where $P_o$ is open porosity (%), $m_{ds}$ is mass of dried sample (g), $m_{inH_2O}$ is mass of sample immersed in water (g), $m_{ms}$ is mass of the moistened sample (g), $V$ is sample volume ($cm^3$), $dp$ is apparent density calculated on the basis of hydrostatic weighing (g $cm^{-3}$), and $N_w$ is water absorption (%).

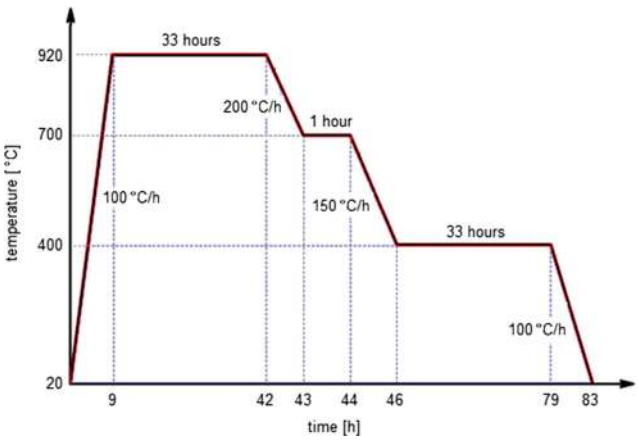


**Fig. 4** Curve of the annealing process in oxygen atmosphere [14]

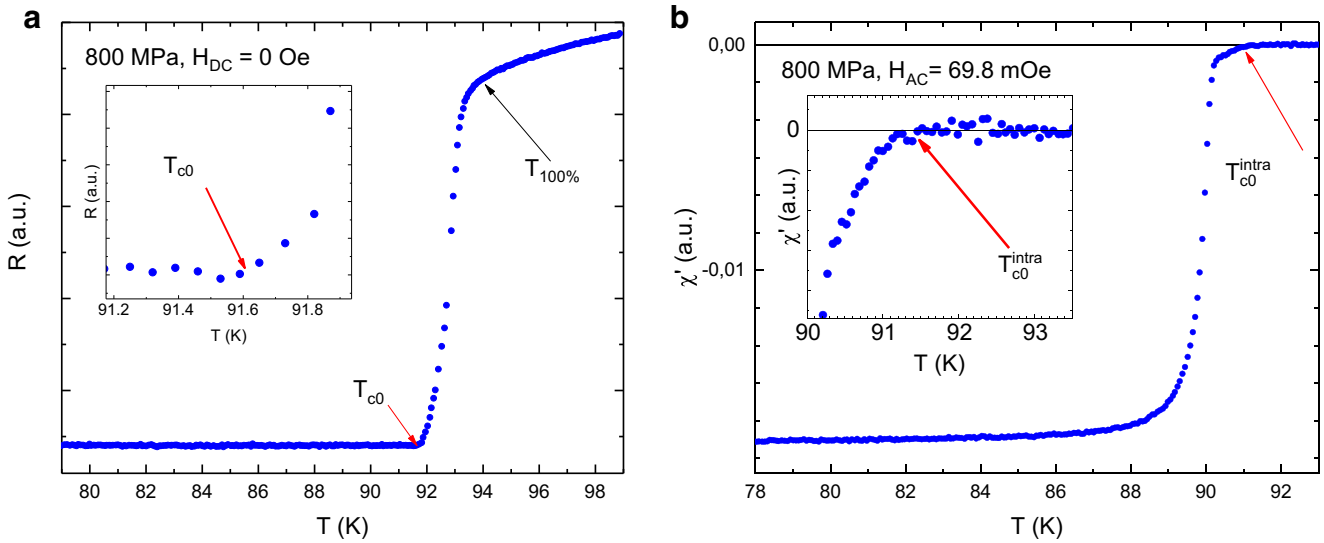


**Fig. 5** **a** Resistance in the function of temperature with shown critical temperature $T_{c0}$. **b** Dispersive component of magnetic dynamic susceptibility in the function of temperature with shown critical temperature $T_c^{intra}$

Qualitative and quantitative phase analysis of the calcined powders and post-annealing materials was performed by X-ray diffraction (XRD) in Bragg-Brentano configuration on a diffractometer equipped with a copper anode lamp. The diffractometer's optical system was composed of a 0.3-in. divergence slot, a 1.50° anti-scatter slot, two 2.5° Soller slots, a Ni filter and a LynxEye strip detector with 2.94° field of view. Quantitative analysis was carried out using the Rietveld method in the Topas v.50 software, based on published crystalline structures (COD and PDF+2014, including ICSD).

Initial powder morphology and material microstructure investigations were performed using SEM with field emission using a low-energy electron beam detector, with energies less than 50 keV, striking electrons from atoms near the surface of the sample. For documenting purposes, raw material photos were taken with magnifications of ×10,000 and samples tested with magnifications of ×5000.

Measurements of AC magnetic susceptibility in the function of temperature and intensity of the AC magnetic field $H_{AC}$ were made using an inductive bridge consisting of a transmission coil and two detector coils set up in the helium cryostat. An SRS830 Lock-In amplifier was used as a detector and the AC current source at 189 Hz. The LakeShore 330 temperature controller was used to control the temperature. The control of the measurements and data acquisition was performed with a PC with appropriate software. The above apparatus was also used to measure the resistance by the four-point method. Resistance was measured as a function of the temperature and the intensity of the external DC magnetic field $H_{DC}$. DC magnetic field was produced in a classic copper coil powered by the Glassman Europe Limited LV 20–50 DC Power Supply. The direction of the magnetic field was parallel to the longest side of the parallelepipedal sample and parallel to the current direction.

Specific resistances of round-shaped pellets of thickness $d$ were determined at room temperature using the van der Pauw method [24, 25] in accordance with the following formula

$$\rho = \frac{\pi d}{\ln 2} \frac{R_{MN,OP} + R_{NO,PM}}{2} \quad (5)$$

**Table 3** The results of XRD-phase analysis obtained after one and two reactions in solid phase

| Crystalline phase | Phase content (wt.%) | |
|---|---|---|
| | After one reaction solid phase | After two reaction solid phase |
| $YBa_2Cu_3O_{7-x}$ | 54.9 ± 0.6 | 93.2 ± 0.6 |
| $BaCuO_2$ | 1.8 ± 0.2 | 2.8 ± 0.2 |
| $BaCO_3$ | 11.9 ± 0.2 | 1.5 ± 0.2 |
| Tenorite | 13.8 ± 0.3 | – |
| $Y_2BaCuO_5$ | 10.4 ± 0.2 | 2.5 ± 0.2 |
| $Ba_2Cu(OH)_6$ | 7.3 ± 0.3 | – |

**Table 4** Average dimensions of YBCO samples formed under different pressures and annealed in oxygen

| Sample | Diameter $\Phi$ (mm) | Thickness $h$ (mm) |
|---|---|---|
| 200A | 11.11 (0.11) | 2.24 (0.10) |
| 400A | 11.14 (0.06) | 2.16 (0.08) |
| 600A | 11.27 (0.02) | 2.12 (0.09) |
| 800A | 11.30 (0.03) | 1.96 (0.07) |
| 200B | 11.04 (0.12) | 6.59 (0.09) |
| 400B | 11.17 (0.06) | 5.83 (0.07) |
| 600B | 11.30 (0.03) | 5.73 (0.07) |
| 800B | 11.43 (0.03) | 5.48 (0.06) |

where $d$ is thickness of sample, $f$ is coefficient whose value depends on $R_{\mathrm{MN,OP}}/R_{\mathrm{NO,PM}}$ ratio.

The resistances $R_{\mathrm{MN,OP}}$ and $R_{\mathrm{NO,PM}}$ were calculated according to formulas:

$$R_{\mathrm{MN,OP}} = \frac{V_{\mathrm{P}} - V_{\mathrm{O}}}{i_{\mathrm{MN}}}, \tag{6}$$

$$R_{\mathrm{NO,PM}} = \frac{V_{\mathrm{M}} - V_{\mathrm{P}}}{i_{\mathrm{NO}}}, \tag{7}$$

where by M, N, O and P are voltage and current contacts that are arranged symmetrically (every 90°) on the circumference of the sample.

The Zero Field Cooling (ZFC) temperature measurements of the dependence of resistance and the dispersive part of the magnetic susceptibility allowed for the determination of the critical temperatures of the superconductive transition which were marked, respectively, by $T_{\mathrm{c0}}$ and $T_{\mathrm{c}}^{\mathrm{intra}}$. $T_{\mathrm{c}}^{\mathrm{intra}}$ was determined as the temperature at which the diamagnetic signal from the sample faded. $T_{\mathrm{c0}}$ was determined as the temperature at which the increase of the measured voltage drop on the sample meets the criterion $E = 10^{-6}$ V cm$^{-1}$ (Fig. 5), where $E$ is the intensity of the electric field. The superconducting transition width $\Delta T$ was determined from the following relationship:

$$\Delta T = T_{90\%} - T_{10\%} \tag{8}$$

wherein $T_{90\%}$ and $T_{10\%}$ are the temperatures where the resistance drop is equal to 90 and 10% of the value of resistance in the temperature at which the superconducting transition beginning was assumed and indicated by $T_{100\%}$. For all the samples measured, the $T_{100\%}$ value was estimated at 94 ± 0.2 K.

The superconducting transition width $\Delta T$ increases with the increasing intensity of the external magnetic field and is described by the following relation [26, 27]:

$$\Delta T\,(H) = C H^{m} + \Delta T_0 \tag{9}$$

where $\Delta T_0$ is the superconducting transition width in zero magnetic field and $C$ is the coefficient that depends on the critical current density value in zero external magnetic field and the critical temperature value and $m$ is the exponent whose value is also related to the properties of the tested superconductor. The density of the intergranular critical current was calculated from the measurements of the absorption part of the AC susceptibility on the basis of Bean's critical condition model [28, 29] and the Ginzburg-Landau strong coupling limit approach [30]. Critical current density $J_{\mathrm{c}}$ for a flat sample with thickness $d$, located in a AC magnetic field with intensity $H_{\mathrm{AC}}$ and parallel to the long side, one can describe as:

$$J_{\mathrm{c}} = 2H_{\mathrm{AC}}/d. \tag{10}$$

In the case of annealed superconductors, one can distinguish two types of critical currents, related to the

**Table 5** The measured and calculated values and of apparent density, open porosity and water absorption of A and B samples

| Sample | $m_{\mathrm{ds}}$ (g) | $m_{\mathrm{inH_2O}}$ (g) | $m_{\mathrm{ms}}$ (g) | $d$ (g cm$^{-3}$) | $p_0$ (%) | $N_{\mathrm{w}}$ (%) |
|---|---|---|---|---|---|---|
| 200A | 1.010 | 1.060 | 0.842 | 4.626 | 22.82 | 4.92 |
| 400A | 0.972 | 1.013 | 0.809 | 4.760 | 19.98 | 4.19 |
| 600A | 0.953 | 0.987 | 0.798 | 5.036 | 17.74 | 3.51 |
| 800A | 0.971 | 1.002 | 0.811 | 5.073 | 16.30 | 3.20 |
| 200B | 2.882 | 2.974 | 2.342 | 4.450 | 24.03 | 5.39 |
| 400B | 2.978 | 3.078 | 2.484 | 4.999 | 20.78 | 4.35 |
| 600B | 2.951 | 3.068 | 2.479 | 5.000 | 19.90 | 3.97 |
| 800B | 2.981 | 3.073 | 2.491 | 5.106 | 15.93 | 3.11 |

$m_{\mathrm{ds}}$, the weight of dry sample; $m_{\mathrm{ms}}$, the wet weight of the sample weighed in air; $\mathrm{m_{inH_2O}}$, the wet weight of the sample weighed in water; $d$, apparent density; $p_0$, open porosity; $N_{\mathrm{w}}$, water absorption

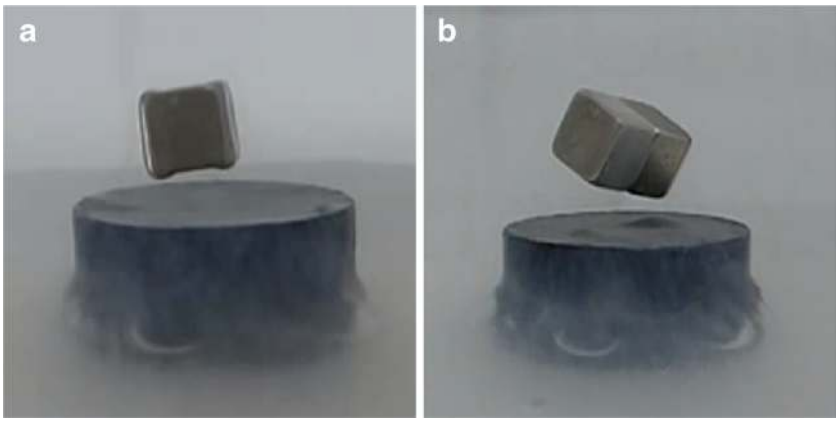


**Fig. 6** Observation of Meissner-Ochsenfeld phenomenon for samples of YBCO high-temperature superconductor: **a** one 1.5 × 1.5 × 1.5 mm magnet placed above the sample and **b** two 1.5 × 1.5 × 1.5 mm magnets placed above the sample

superconducting properties of the superconductor grains and to intergranular connections. The density of critical currents of integranular connections is several orders of magnitude less than the density of internal grain currents and, for example, for YBCO-123 superconductors is about 500 A $cm^{-2}$ [31]. In AC magnetic susceptibility measurements, we typically measure the properties of weaker, intergranular connections. From Ginzburg-Landau approximation, the critical current density in the function of temperature is given by:

$$J\,(T) = J_{c0}\left(1 - \frac{T}{T_{c0}}\right)^{n}, \tag{11}$$

where $T_{c0}$ is the critical temperature of the intergranular connections for $H_{AC} = 0$, $J_{c0}$ is the critical current density

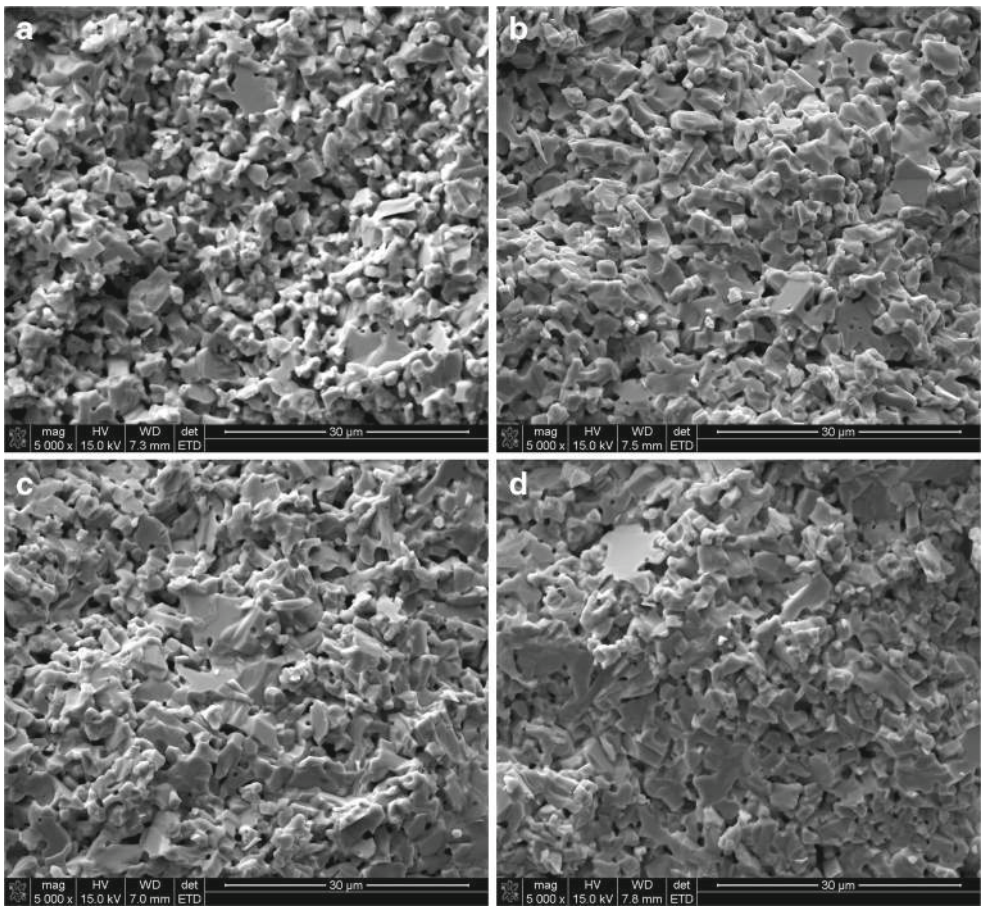


**Fig. 7** Example SEM images (magnification, ×5000) of the microstructure of YBCO samples pressed under pressure: **a** 200, **b** 400, **c** 600 and d 800 MPa

**Table 6** Quantitative XRD-phase analysis of YBCO samples

| Crystalline phase | Phase content (wt.%) | | | |
|---|---|---|---|---|
| | 200 MPa | 400 MPa | 600 MPa | 800 MPa |
| $YBa_2Cu_3O_{6.83}$ | 97.0 ± 0.6 | 97.3 ± 0.7 | 96.9 ± 0.6 | 97.1 ± 0.6 |
| $BaCuO_2$ | 2.0 ± 0.3 | 2.7 ± 0.3 | 3.1 ± 0.3 | 3.0 ± 0.3 |

at 0 K, $n$ is the exponent whose value can be associated with the value of exponent $m$ in formula (9) with $n = 1/m$.

## 5 Results of Research

### 5.1 XRD Phase Analysis of Calcined Powders

The results of XRD phase analysis obtained after one and two reactions in solid phase are presented in Table 3. These results clearly indicate that the material after two reactions contained smaller amounts of some undesirable phases, such as $BaCO_3$ and $Y_2BaCuO_5$. On the other hand, others—like tenorite and $Ba_2Cu(OH)_6$—were not present at all.

### 5.2 Study of Physical Properties

Table 4 provides the data on the dimensions and weight of the samples compacted at different pressures (200, 400, 600 and 800 MPa) and annealed in oxygen. The results indicate that for both sample groups, as the pressure increases, the diameter increases and the sample thickness decreases. Decreasing of the thickness of the samples indicates a progressive increase in sample density with increasing forming pressure. In contrast, the increase in diameter is due to internal stresses of pressing and the phenomenon of expansion of the sample when it is pushed out of the mold. As the pressure of the pressing increases, the internal stresses in the sample increase, which results in a higher expansion.

In order to assess the physical properties of samples annealed in oxygen, their apparent density, open porosity and water absorption were determined by hydrostatic weighing. The results of the study are shown in Table 5.

On the basis of the results in Table 5, it can be seen that with increasing forming pressure, the apparent density increases, while the open porosity and water absorption decrease. This proves that the forming pressure affects the degree of densification of the samples.

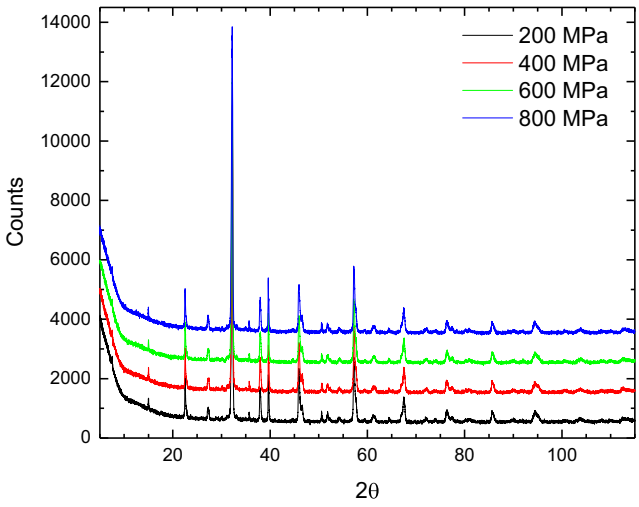


**Fig. 8** X-ray diffraction patterns of samples (series A) pressed at 200, 400, 600 and 800 MPa

### 5.3 Meisner-Ochsenfeld Phenomenon

To verify that the samples obtained are high-temperature ceramic superconductors, a pre-test for the Meisner-Ochsenfeld phenomenon has been performed. By immersion in liquid nitrogen, the samples were cooled to the boiling point of liquid nitrogen (77 K). A magnet weighing about 1 g was placed above the sample. The observed levitation of the magnet over the sample of YBCO material confirmed the superconductivity of the samples obtained (Fig. 6).

### 5.4 Observations of Microstructure

Microscopic observations were made using a scanning microscope that did not show any significant differences

**Table 7** Resistivity at room temperature and critical temperature values. $T_{c0}$ ($H_{DC} = 0$) is critical temperature determined from resistance measurements in the function of temperature. $T_c^{intra}$ is critical temperature determined from the dispersion part of AC magnetic susceptibility in the function of temperature

| Sample (MPa) | $\rho$ (300 K) (μΩcm) | $T_{c0}$ (K) | $T_c^{intra}$ (K) |
|---|---|---|---|
| 200 | 2100 ± 100 | 91.4 ± 0.3 | 91.7 ± 0.3 |
| 400 | 2000 ± 100 | 91.4 ± 0.3 | 91.6 ± 0.3 |
| 600 | 1500 ± 100 | 91.5 ± 0.3 | 91.5 ± 0.3 |
| 800 | 2000 ± 100 | 91.6 ± 0.3 | 91.6 ± 0.3 |

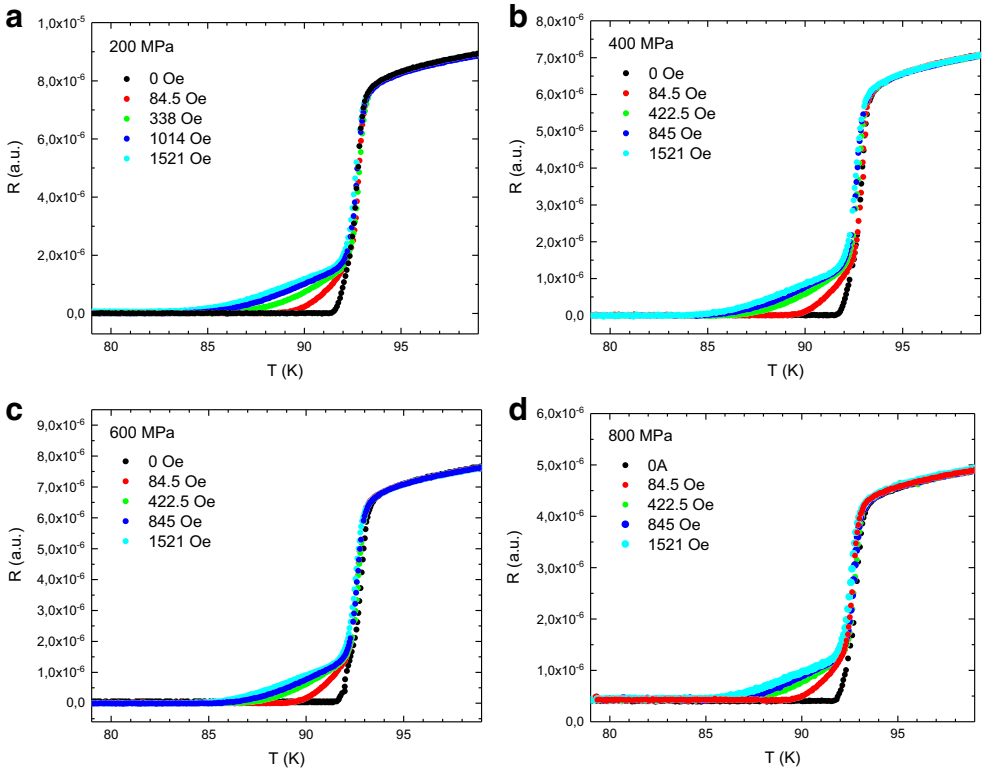


**Fig. 9** Selected resistance measurements in the function of temperature and the intensity of the $H_{DC}$ magnetic field for samples: **a** 200, **b** 400, **c** 600 and **d** 800 MPa

in either grain size or integranular space depending on the forming pressure (Fig. 7).

### 5.5 Phase Analysis of the Material

The obtained YBCO superconductor samples were subjected to phase tests. The A series samples were selected for the study. The quantitative analysis of the phase content was carried out using the Rietveld method in the Topas v.50 software based on published crystalline structures (COD and PDF+2014, including ICSD). The results of the quantitative analysis are shown in Table 6. The analysis showed that the samples were mainly obtained with a rhombohedral phase of $YBa_2Cu_3O_{6.83}$ (where $x = 0.17$) and a small amount of $BaCuO_2$ phase. Oxygen factor $x$ was the fitting parameter in Rietved refinement procedure utilised in the Topas v.50

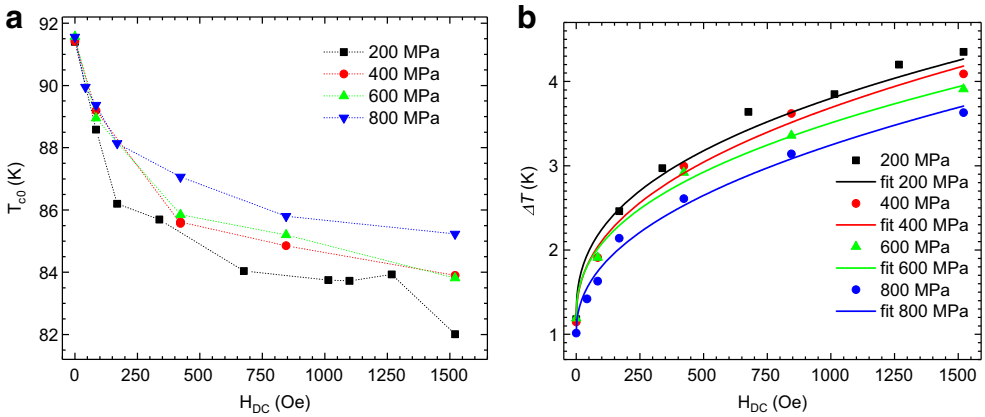


**Fig. 10** Results of magnetoresistance measurements: **a** critical temperature $T_{c0}$. The dotted lines are only a guide to the eye; **B** superconducting transition width $\Delta T$ in function of $H_{DC}$. The fit results to relationship (9) are shown as solid lines

**Table 8** Fitting results of $\Delta T$ to relationship (9)

| Sample (MPa) | $C$ | $m$ | $\Delta T_0$ (K) |
|---|---|---|---|
| 200 | $0.18 \pm 0.19$ | $0.39 \pm 0.16$ | 1.2 |
| 400 | $0.14 \pm 0.04$ | $0.42 \pm 0.04$ | 1.2 |
| 600 | $0.13 \pm 0.03$ | $0.42 \pm 0.03$ | 1.2 |
| 800 | $0.10 \pm 0.02$ | $0.45 \pm 0.03$ | 1.0 |

$\Delta T_0$ is the superconducting transition width for $H_{DC} = 0$

software. Phase analysis did not show the dependence of the content of superconducting—rhombohedral—phase on the pressure of sample pressing.

The X-ray diffraction patterns for the samples obtained at different pressures are given in Fig. 8. The diffractograms show clear peaks confirming the presence of the rhombohedral $YBa_2Cu_3O_{6.83}$ phase.

### 5.6 Specific Resistance and Dependence of Resistance on Temperature and Magnetic Field

The testing of the superconducting properties of the samples was carried out on the basis of the results of magnetoresistance measurements and of the AC magnetic susceptibility in the function of the temperature and intensity of the external magnetic field $H_{DC}$.

The results of the measurement of resistivity in room temperature $\rho$ (300 K) with the use of the van der Pauw method are presented in Table 7. The obtained values of $\rho$ (300 K) are about 2 mΩcm (2000 μΩcm) and are typical of polycrystalline superconductors prepared with the use of the solid-state reaction method [32, 33]. There is no apparent relationship between the $\rho$ (300 K) value and the sample forming pressure.

The dependence of the resistance in function of the temperature and the external magnetic field $H_{DC}$ is shown in Fig. 9. Based on the magnetoresistance measurements for each sample, the critical temperature $T_{c0}$ and the superconducting transition width $\Delta T$ were determined. The determined values are shown in the function of the field strength $H_{DC}$ in Fig. 9 and are summarised in Table 7.

Critical temperature $T_{c0}$ for all samples decreases as the intensity of the external magnetic field $H_{DC}$ increases and the superconducting transition width $\Delta T$ grows. A positive effect of forming pressure on the samples of $\Delta T$ and $T_{c0}$ can be observed. Samples that were pressed at a higher pressure have a higher critical temperature $T_{c0}$ and a narrower superconducting transition $\Delta T$. With the increasing intensity of the $H_{DC}$ field, the differences between $T_{c0}$ and $\Delta T$ are increasing.

The result of the fit of the superconducting transition width $\Delta T$ $(H)$ to relationship (9) is shown in Fig. 10b. The determined values of parameters $C$, $m$ and $\Delta T_0$ are shown in Table 8. For all samples, the value of the exponent $m$ is less than the theoretical value $m = 2/3$, which, according to the interpretation in Woch et al. [34] points to a more two-dimensional structure of the vortexes in the samples tested and a high pinning force, which will present itself as a high critical current density.

### 5.7 The Dependence of Magnetic Susceptibility on Temperature

The results of the measurements of the AC magnetic susceptibility in the function of the temperature and amplitude of the magnetic field $H_{AC}$ from 26 mOe to 10.9 Oe are shown in Fig. 11.

The measurements of the dispersion component of the AC magnetic susceptibility allowed for the determination of the values of the critical temperatures $T_c^{intra}$ of grains. Within the tested range of the magnetic field intensity $H_{AC}$, these temperatures do not depend on the amplitude $H_{AC}$, and they are 91.7, 91.6, 91.5 and 91.6 K, respectively, for samples 200, 400, 600 and 800 MPa (Table 7). The uncertainty of the determined temperature was estimated to be 0.3 K. The indicated temperatures $T_c^{intra}$ of the grains are consistent with literature reports obtained for good-quality YBCO samples.

In the measurements of the absorption part of AC magnetic susceptibility, a single absorption peak was observed for all samples. The peak appears due to energy losses connected with the magnetic field penetration into the intergranular regions. For small $H_{AC}$ field strengths, intergranular absorption peak appears approximately 1.5–2 K below $T_c^{intra}$ of the sample. With the increase in $H_{AC}$, the location of the peak on the temperature axis is shifted towards lower temperatures. For the maximum value of $H_{AC} = 10.9$ Oe, the absorption peak were approximately 86 K for all samples. No absorption peak was observed for the magnetic field penetration into grains, which, if visible, is slightly below the critical temperature $T_c^{intra}$.

### 5.8 Critical Current Density

Figure 12 shows the value of critical current density of intergranular connections in the function of temperature, calculated according to dependence (10) and their fit to dependence (11). The determined values of fitting parameters $J_{c0}, T_{c0}, n$ and the estimated values of the critical current density at liquid nitrogen temperature $J_c$ (77 K) are shown in Table 9. 86–90 K temperature range, where the position of the intergranular absorption

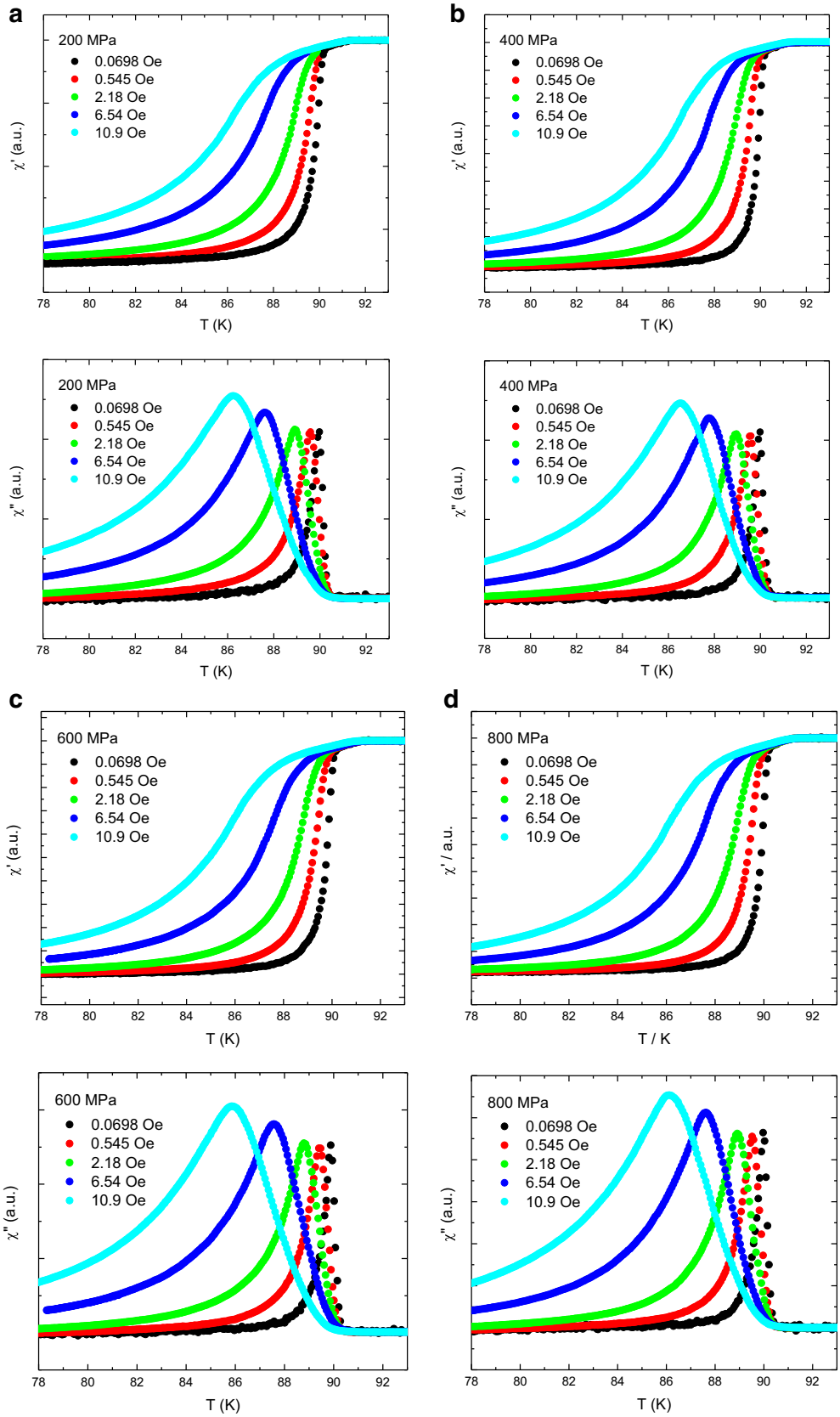


**Fig. 11** Normalised dispersion $\chi'$ and absorption $\chi''$ components of dynamic magnetic susceptibility and selected $H_{AC}$ amplitudes for samples: **a** 200, **b** 400, **c** 600 and **d** 800 MPa

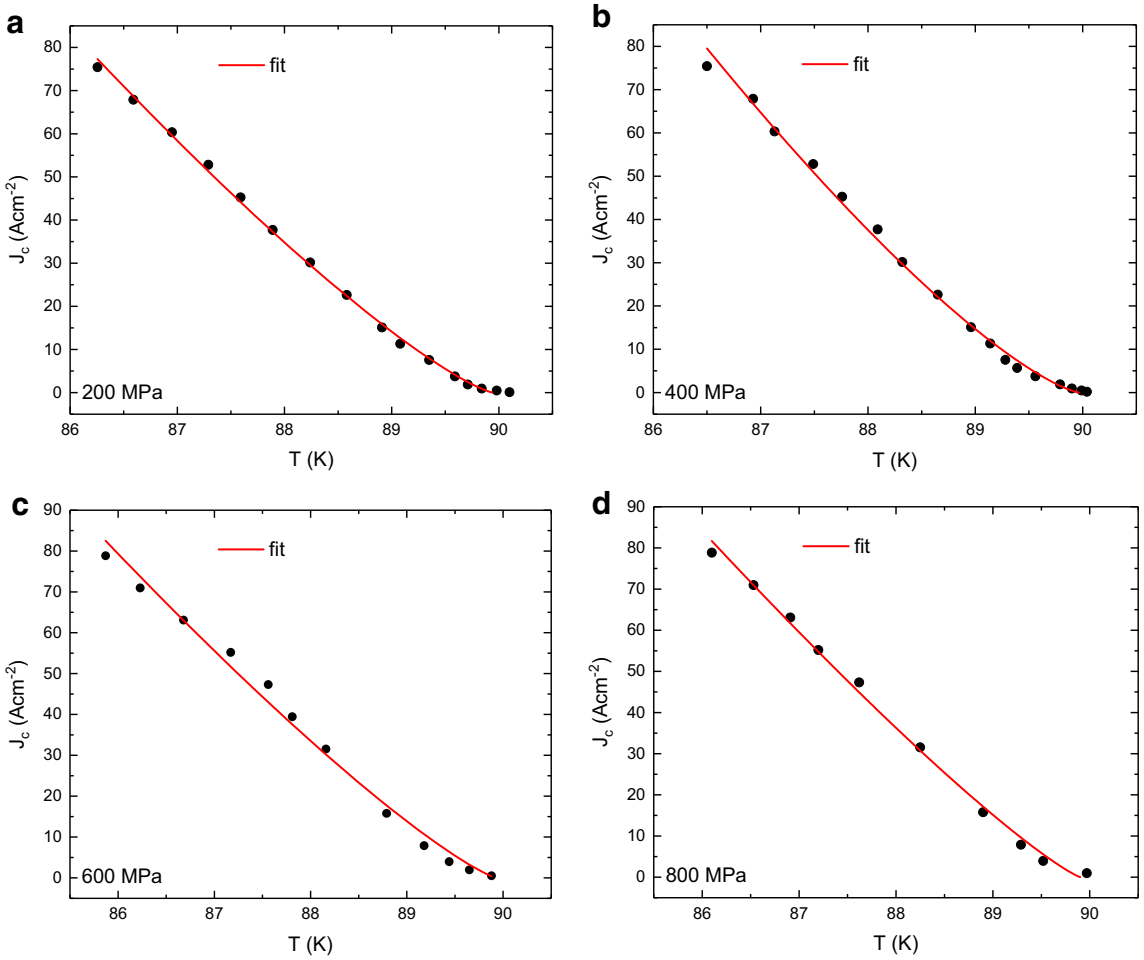


**Fig. 12** Critical current density $J_c$ in the function of temperature and its fit to relationship (11) for samples: **a** 200, **b** 400, **c** 600 and **d** 800 MPa

maxima were observed and analysed, the values of the critical current densities of the samples were similar (Fig. 13) which cannot be said of the calculated values of $J_c$ (77 K) of samples. $J_c$ (77 K) non-monotonically varies in the range from 335 to 455 A cm$^{-2}$. Despite this fact, the estimated values of $J_c$ (77 K) are typical for polycrystalline superconductors prepared with the use of the solid-phase reaction method. The large dispersion of $J_c$ (77 K) values between samples results mainly from the high impact of the errors of temperature measurement on the fit values of the parameters $J_{c0}$, $T_{c0}$ and $n$.

**Table 9** The results of fit $J_c$ ($T$) to dependence (11)

| Sample (MPa) | $J_{c0}$ (A cm$^{-2}$) | $T_{c0}$ (K) | $n$ | $J_c$ (77 K) (A cm$^{-2}$) |
|---|---|---|---|---|
| 200 | 4120 ± 580 | 89.94 ± 0.04 | 1.24 ± 0.05 | 370 |
| 400 | 5900 ± 1600 | 89.97 ± 0.07 | 1.32 ± 0.08 | 460 |
| 600 | 3510 ± 800 | 89.93 ± 0.08 | 1.21 ± 0.07 | 340 |
| 800 | 3300 ± 1000 | 89.90 ± 0.10 | 1.20 ± 0.10 | 340 |

$T_c$, $n$ and $J_{c0}$ are fit parameters

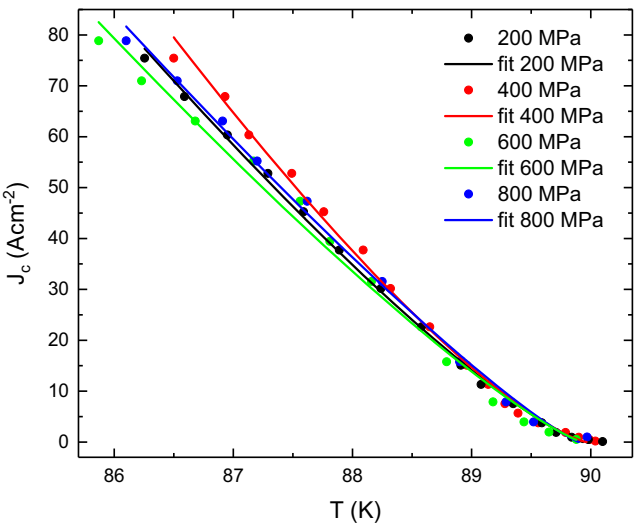


**Fig. 13** Comparision of samples critical current densities $J_c$ according to the dependency (10) and the fit to the relationship (11)

## 6 Summary

By solid-state reaction method, single-phase samples of superconductive $YBa_2Cu_3O_{6.83}$ (rhombohedric phase) were obtained with a very small amount of $BaCuO_2$ phase. No dependence of the content of the superconducting (rhombohedral) phase on the sample-forming pressure was found.

The microstructure of the samples observed using a scanning electron microscope did not show any significant differences in either grain size or intergranular spaces depending on the pressing conditions.

The pressing pressure has an effect on the degree of density of the samples. As the pressure increases, the apparent density of the samples increases, while their open porosity and water absorption decrease.

Resistivity at room temperature $\rho$ (300 K) was determined by the van der Pauw method. The obtained values at $\rho$ (300 K) are about 2000 μΩcm and are typical of polycrystalline superconductors prepared with the use of the solid-state reaction method.

Value of critical temperature $T_{c0}$ in self magnetic field ($H_{DC} = 0$) does not depend on the forming pressure and is 91.4, 91.4, 91.5 and 91.6 K for samples 200, 400, 600 and 800 MPa, respectively. The $T_{c0}$ uncertainty was estimated as 0.3 K.

In the external magnetic field $H_{DC}$, all samples showed a decrease in the critical temperature $T_{c0}$ and increase in the width of the superconducting transition $\Delta T$ along with increasing intensity of the $H_{DC}$ filed increases. Samples pressed at higher pressures show smaller changes of $T_{c0}$ and $\Delta T$ caused by $H_{DC}$ field than the samples pressed at lower pressures.

The analysis of the superconducting transduction width $\Delta T$ in the function of the external magnetic field showed that the samples are characterised by a more two-dimensional structure of the vortexes.

The measurements of the dispersion component of the AC magnetic susceptibility allowed for the determination of the values of the critical temperatures $T_c^{intra}$ of grains. Within the tested range of the varying magnetic field intensity $H_{AC}$ (0–10.9 Oe), these temperatures do not depend on the amplitude $H_{AC}$, and they are 91.7, 91.6, 91.5 and 91.6 K for samples 200, 400, 600 and 800 MPa, respectively. The $T_c^{intra}$ uncertainty was estimated as 0.3 K.

The critical current density $J_c$ (77 K) varies within the range from 340 to 460 A $cm^{-2}$, does not depend on the forming pressure and is typical for polycrystalline superconductors prepared with the use of the solid-phase reaction method.

The determined critical temperatures $T_c^{intra}$ and $T_{c0}$, critical current density $J_c$ (77 K) have values very similar to the results reported in the literature for good-quality YBCO samples prepared with the use of the solid-phase reaction method.



## References

1. Wu, M.K., Ashburn, J.R., Torng, C.J., Hor, P.H., Meng, R.L., Gao, L., Huang, Z.J., Wang, Y.Q., Chu, C.W.: Superconductivity at 93 K in a new mixed-phase Y-Ba-Cu-O compound system at ambient pressure. Phys. Rev. Lett. **58**(9), 908–910 (1987)
2. Maeda, H., Tanaka, Y., Fukutomi, M., Asano, T.: A new high-r. oxide superconductor without a rare earth element. Jpn. J. Appl. Phys. **2**(27), L209–10 (1988)
3. Sheng, Z.Z., Hermann, A.M.: Superconductivity in the rare-earth-free Tl–Ba–Cu–O system above liquid-nitrogen temperature. Nature **332**, 55–58 (1988)
4. Karpiński, J., Kaldis, E., Jilek, E., Rusiecki, S., Bucher, B.: Bulk synthesis of the 81 K superconductor $YBa_2Cu_4O_8$ at high oxygen pressure. Nature **336**, 660–662 (1988)
5. Putilin, S.N., Antipov, E.V., Chmaissem, O., Marezio, M.: Superconductivity at 94 K in $HgBa_2Cu0_{4+\delta}$. Nature **362**, 226–228 (1993)
6. Kawashima, T., Matsui, Y., Takayama-Muromachi, E.: New oxycarbonate superconductors $(Cu_{0.5}C_{0.5})Ba_2Ca_{n-1}Cu_nO_{2n+3}$ (n=3,4) prepared at high pressure. Physica C **224**, 69–74 (1994)
7. Schwartz, J., Amm, K.M., Sun, Y.R., Wolters, C.: HgBaCaCuO superconductors: processing, properties and potential. Physica B **216**(3–4), 261–265 (1996)
8. Chu, C.W., Hor, P.H., Meng, R.L., Gao, L., Huang, Z.J., Wang, Y.Q.: High-pressure study of the new Y-Ba-Cu-O superconducting compound system. Phys. Rev. Lett. **58**, 911–912 (1987)
9. Rymaszewski, J., Lebioda, M.: Nadprzewodniki YBaCuO o zmodyfikowanej stechiometrii. Prace Instytutu Elektrotechniki **261**, 58–65 (2013)
10. Paturi, P., Raittila, J., Grivel, J.C., Huhtinen, H., Seifi, B., Laiho, R., Andersen, N.H.: Preparing superconducting nanopowder based YBCO/Ag tapes. Physica C **372–376**, 779–781 (2002)
11. Onabe, K., Doi, T., Kashima, N., Nagaya, S., Saitoh, T.: Preparation of $Y_1Ba_2Cu_3O_x$ superconducting tape formed on silver substrate by chemical vapor deposition technique. Physica C **378–381**, 907–910 (2002)
12. Ruckenstein, E., Narain, S., Wu, N.J.: Reaction pathways for the formation of the $YBa_2Cu_3O_{7-x}$. J. Mater. Res. **4**(2), 267–272 (1989)
13. Pathak, L.C., Mishra, S.K.: A review on the synthesis of Y-Ba-Cu-O powder. Supercond. Sci. Technol. **18**(9), R67–R89 (2005)
14. Alagöz, S.: Production of YBCO superconductor sample by powder-in-tube method (PITM) and effect of Cd and Ga doping on the system. Turk. J. Phys. **33**, 69–80 (2009)
15. Pęczkowski, P., Szterner, P., Jaegermann, Z.: Ceramic high-temperature superconductors—division and application. Prace ICiMB **27**, 57–70 (2016)
16. Szterner, P., Pęczkowski, P., Jaegermann, Z.: Ceramic high-temperture superconductors—preparation of $YBa_2Cu_3O_{7-x}$ by calcination methods. Prace ICiMB **28**, 62–75 (2017)
17. Ohmukai, M.: The effect of the pressure for the formation of $YBa_2Cu_3O_{7-d}$bulk ceramics with domestic microwave oven. Engineering **3**, 1095–1097 (2011)
18. Rha, J.J., Yoon, K.J., Kang, S.J.L., Yoon, D.N.: Rapid calcination and sintering of $YBa_2Cu_3O_x$superconductor powder mixture in inert atmosphere. J. Am. Ceram. Soc. **71**(6), C328–C329 (1988)

19. Ruckenstein, E., Wu, N.: A two-step calcination method for preparing $YBa_2Cu_3O_{7-x}$ powders. Mater. Lett. **7**(5–6), 165–168 (1988)
20. Uno, N., Enomoto, N., Tanaka, Y., Takami, H.: Synthesis of superconductive oxides by vacuum calcination method. Jpn. J. Appl. Phys. **27**(2(6)), 1003–1006 (1988)
21. Lay, K.W.: Formation of yttrium barium cuprate powder at low temperatures. J. Am. Ceram. Soc. **72**(4), 696–698 (1989)
22. Schartman, R.R., Hellstorm, E.E.: The low-temperature synthesis of $YBa_2Cu_3O_{7-\delta}$under reduced oxygen pressure. Physica C **173**(3–4), 245–250 (1991)
23. Al-Shibani, K., Al-Aql, A., Al-Muezzin, A., Humeida, H., Nakhmedov, E.P., Firat, T., Öztürk, O., Sacli, Ö.A.: Effect of forming pressure on the critical temperature in $YBa2Cu3O_{7-x}$ superconductors. Phys. Stat. Sol. B **189**, 177–184 (1995)
24. Van der Pauw, L.J.: A Method of measuring the resistivity and Hall coefficient on lamellae of arbitrary shape. Philips Tech. Rev. **26**, 220–224 (1958)
25. Van der Pauw, L.J.: A method of measuring specific resistivity and Hall effect of discs of arbitrary shape. Philips Res. Rep. **13**, 1–9 (1958)
26. Woch, W.M., Zalecki, R., Kołodziejczyk, A., Chmist J., Heiml O., Gritzner G.: Effect of magnetic field on resistive transition of thin film thallium based superconductors. Acta Phys. Pol. A **106**, 785–791 (2004)
27. Woch, W.M., Zalecki, R., Kołodziejczyk, A., Sudra, H., Gritzner G.: Properties, magnetic susceptibility, critical currents and irreversibility fields of $(Tl_{0.5}Pb_{0.5})Sr_2(Ca_{1-x}Gd_x)Cu_2O_z$ bulk superconductors. Supercond. Sci. Technol. **21**, 085002–85008 (2008)
28. Bean, C.P.: Magnetization of hard superconductors. Phys. Rev. Lett. **8**, 25–253 (1962)
29. Clem, J.R.: Granular and superconducting-glass properties of the high-temperature superconductors. Physica C **153–155**, 50–55 (1988)
30. Clem, J.R., Bumble, B., Raider, S.I., Gallagher, W.J., Shih, Y.C.: Ambegaokar-Baratoff—Ginzburg-Landau crossover effects on the critical current density of granular superconductors. Phys. Rev. B **35**, 6637–6642 (1987)
31. Cyrot, M., Pavuna, D.: Introduction to Superconductivity and High-$T_c$-Materials. World Scientific in Singapore, River Edge (1992)
32. Kujur, A.: Effect of various pinning centers on electric and magnetic transport properties in $YBa_2Cu_3O_{7-\delta}$. PhD thesis, Department of Physics and Astronomy National Institute of Technology Rourkela Odisha, India (2014)
33. Nishio, T., Itoh, Y., Ogasawara, F., Suganuma, M., Yamada, Y., Mizutani, U.: Superconducting and mechanical properties of YBCO-Ag composite superconductors. J. Mater. Sci. **24**, 3228–3234 (1989)
34. Woch, W.M., Chrobak, M., Kowalik, M., Zalecki, R., Przewoźnik, J., Kapusta, C.: Magnetoresistance and irreversibility fields of bismuth-based 1G tape. J. Supercond. Nov. Magn. **29**, 2333–2336 (2016)